Unexpectedly wide reversible vortex region in β-pyrochlore $RbOs_2O_6$: Bulk magnetization measurements

Pierre Legendre, Yanina Fasano, Ivan Maggio-Aprile, and Øystein Fischer
Département de Physique de la Matière Condensée, Université de Genève, 24 Quai Ernest-Ansermet, 1211 Geneva, Switzerland

Zbigniew Bukowski, Sergiy Katrych, and Janusz Karpinski
Laboratory for Solid State Physics, ETH Zürich, 8093 Zürich, Switzerland

(Received 28 May 2008; revised manuscript received 5 August 2008; published 17 October 2008)

We study the extent of the reversible region in the vortex phase diagram of recently available $RbOs_2O_6$ single crystals [Rogacki *et al.*, Phys. Rev. B **77**, 134514 (2008)] by means of bulk magnetization measurements. We found that the irreversible magnetic response sets in at a field $H_{irr}(T) \sim 0.3H_{c2}(T)$ for $0.5 \lesssim T/T_c \lesssim 0.8$ yielding a reversible vortex region that is wide in comparison with other low-T_c materials. The relevance of thermal fluctuations is limited since we estimate a Ginzburg number $G_i = 5 \times 10^{-7}$. However, the relevance of quenched disorder is low since the critical-current density ratio at low fields and temperatures is of the order of that found in high T_c's. We therefore conclude that an intrinsically low bulk pinning magnitude favors the existence of an unexpectedly wide reversible vortex region in $RbOs_2O_6$.

DOI: 10.1103/PhysRevB.78.144513 PACS number(s): 74.25.Dw, 74.25.Ha, 74.25.Sv

I. INTRODUCTION

The recent discovery of superconductivity in the β-pyrochlore osmate compounds AOs_2O_6 [A=K,[1,2] Rb,[3–5] and Cs (Ref. 6)] triggered a plethora of studies on the superconducting pairing mechanism in these compounds. In spite of the active research on β pyrochlores over the last four years, only three works report on the magnetic and spectroscopic properties of vortex matter in these compounds.[7–9] These three studies focus on KOs_2O_6, the β pyrochlore which presents the highest $T_c \sim 9.6$ K.[10] This compound has a Ginzburg-Landau parameter $\kappa = 70-87$ (Refs. 11 and 12) and $H_{c2}(0) = 24$ (single crystals[11])—33 T (polycrystals[13]) which is larger than the Pauli paramagnetic limiting field.[2] This suggests that at very low temperatures exotic superconducting phases might be stable at high magnetic fields.[2] In the rest of the $H-T$ phase diagram conventional vortex physics is expected.

The first of these works[7] reports a low-field re-entrant behavior of the temperature at which resistance becomes negligible. The re-entrance is detected for vortices moving in particular crystallographic directions. This suggests that the phenomenon has its origin in a pinning mechanism arising from the specific crystal structure of KOs_2O_6 indicating a resemblance to the intrinsic pinning mechanism detected in high-T_c superconductors.[14]

The second of these works[8] reports a drastic change in the spatial distribution of vortices when cooling through a temperature T_p. Specific-heat measurements established that KOs_2O_6 presents a first-order phase transition at an almost field-independent temperature $T_p \sim 8$ K.[7,11] This transition has been associated with the freezing of the "rattling" phonon mode arising from the vibration of the K ion within the oversized Os-O cage.[15] The low-temperature ($T < T_p$) vortex phase is characterized by a reduced vortex line energy[8] implying a decrease in the vortex-vortex interaction energy. This study therefore raises the question of a structural transition in the KOs_2O_6 vortex matter occurring at T_p.

The third of these works[9] reports on scanning tunneling microscopy imaging of vortices in the low-temperature phase. The observed structures present significant variations in the intervortex distances. In particular, the spacing between some vortices is roughly half the average vortex lattice parameter. These findings are in agreement with a reduction in the vortex interaction energy for the phase located at $T < T_p$.

These works suggest that vortex matter in KOs_2O_6 presents unexpected properties for a low-T_c material. Therefore, studies in $RbOs_2O_6$ and $CsOs_2O_6$ are necessary to gain more insight into the properties of vortex matter in the β-pyrochlore osmate family. This is particularly relevant since Rb and Cs β pyrochlores do not present the first-order phase transition associated with a dramatic change in the phonon spectra in the superconducting phase.[16]

In this work we study the vortex phase diagram of $RbOs_2O_6$ single crystals by means of bulk magnetization measurements. Up until now, only one work reports on structural and superconducting properties of $RbOs_2O_6$ single crystals[17] and the rest of the literature is devoted to polycrystalline samples. The most important result reported here is that $RbOs_2O_6$ presents a wide reversible vortex region spanning down to a field $H_{irr}(T) \sim 0.3H_{c2}(T)$ at low temperatures. This finding is in direct contrast with results found in other low-T_c superconductors. We provide evidence that the wide reversible region originates from the small critical-current density in $RbOs_2O_6$. The unusually wide reversible region and the low critical-current density observed in $RbOs_2O_6$ are consistent with the available data for KOs_2O_6.[2]

II. EXPERIMENTAL AND SAMPLE DETAILS

The study presented here was carried out on two $RbOs_2O_6$ single crystals of the same batch that provided similar results. The samples were grown in evacuated quartz ampoules following the method described in Ref. 17. The crystals have a prismlike shape with typical dimensions $0.1-0.2 \times 0.2$

TABLE I. Structure and refinement data for $RbOs_2O_6$ at 295,0(5) K.

Wavelength, Å/radiation	0.71073/Mo $K\alpha$
Crystal system, space group	cubic, Fd-3m (No 227)
Unit cell dimensions, Å	a=10.1214(8)
Volume, Å^3	1036.9(4)
Z	8
Absorption correction type	analytical
Theta range for data collection	5.79° to 36.13°
Limiting indices	$-13 \leq h \leq 12$, $-14 \leq k \leq 10$, $-13 \leq l \leq 13$
Reflections collected/unique	937/94, R_{int}=0.032
Refinement method	Full-matrix least squares on F^2
Data /restraints/parameters	94/0/7
Goodness-of-fit on F^2	1.310
Final R indices [$I>2\sigma(I)$]	R_1=0.0322, wR_2=0.0791
R indices (all data)	R_1=0.0335, wR_2=0.0808
Extinction coefficient	0.0064(7)
$\Delta\rho_{max}, \Delta\rho_{min}(e/Å^3)$	2.890 and −2.408

$\times 0.2$ mm^3 and weight $49.7-100.2 \pm 0.1$ μg.

The structural properties of the crystals were investigated on a four-circle x-ray diffractometer (XCalibur PX of Oxford Diffraction with an oscillation angle of 1° and Mo $K\alpha$ radiation) equipped with a charge-coupled device (CCD) area detector placed at 60 mm from the sample. The data were refined on F^2 by employing the program SHELXL-97 (Ref. 18) and the results reveal a β-pyrochlore cubic structure[19,20] (see Table I). The occupation of all elements remained 100 % during the structural refinement. No additional phases (impurities, twins or intergrowth crystals) were detected by examining the reconstructed reciprocal space section shown in Fig. 1. The crystals present low mosaicity with an average mosaic spread of 0.13(3) (estimated analyzing every frame by using XCalibur with the CRYSALIS software system[21]). The observed reflections present a smaller intensity than the calculated ones (extinction coefficient $\epsilon=64(7)\times 10^{-4}$; see Table I). This can be explained by the very small misorientation of mosaic blocks. The reconstructed reciprocal space section and refinement results indicate that the single crystals used in this study are of a high crystalline perfection.

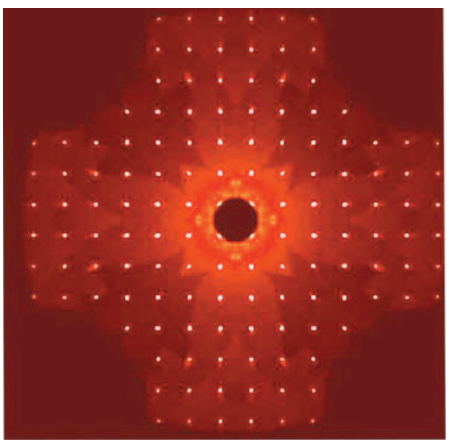

FIG. 1. (Color) Reconstructed $h1l$ reciprocal space section of a $RbOs_2O_6$ sample measured at 295 K.

The superconducting magnetic properties of the samples were characterized by zero-field-cooled (ZFC) and field-cooled (FC) magnetization vs temperature measurements $M(T)$ and magnetization vs magnetic-field loops $M(H)$. Measurements for applied fields below 1.2 T were performed in a superconducting quantum interference device (SQUID) magnetometer; for larger applied fields a physical properties measurement system (PPMS) magnetometer was used.

III. RESULTS AND DISCUSSION

The critical temperature of the samples was determined by resistivity R, ac susceptibility χ', and low-field magnetization M measurements (see Fig. 2). T_c is defined as the

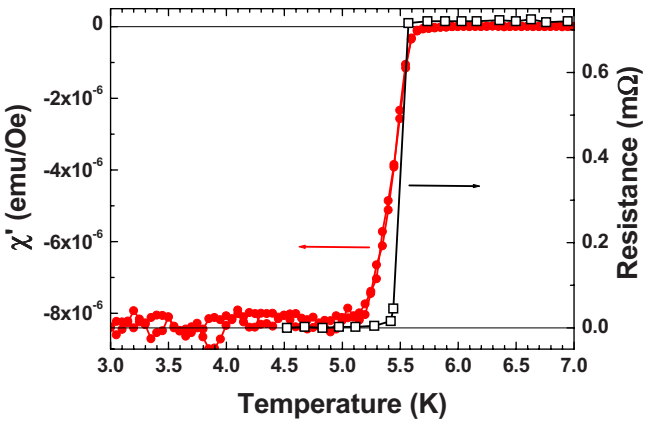

FIG. 2. (Color online) (a) Superconducting transition of one of our $RbOs_2O_6$ crystals at zero field as detected by resistivity (open black symbols) and the real component of the ac susceptibility (full red symbols). ac susceptibility measurements were performed with an applied field of 5 Oe at 970 Hz.

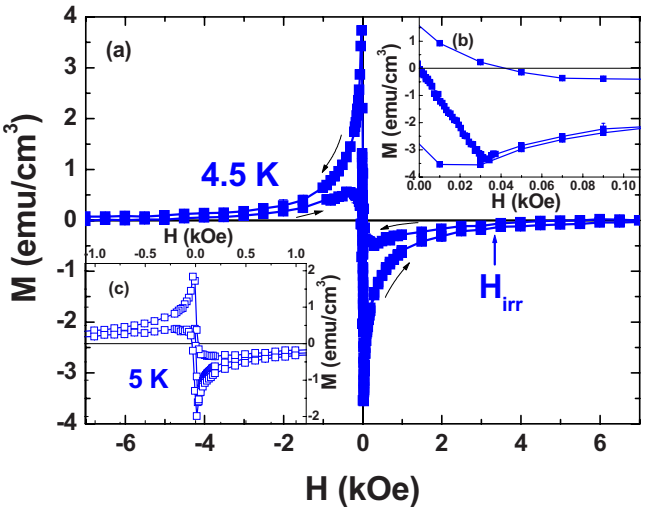

FIG. 3. (Color online) Magnetization vs magnetic-field curves for $RbOs_2O_6$ single crystals. (a) Magnetization loop at 4.5 K. The irreversibility field determined from ZFC-FC $M(T)$ measurements is indicated. (b) Zoom of the magnetization in the low-field region allowing a detailed observation of the Meissner branch. (c) Magnetization loop of $RbOs_2O_6$ at 5 K.

temperature at which $\partial\chi'/\partial T$, $\partial M/\partial T$, and $\partial R/\partial T$ present a peak. The transition width is estimated as the full width at half maximum of these peaks. Critical temperature values of $T_c=(5.50\pm0.05)$ K from resistivity and (5.45 ± 0.03) K from susceptibility and magnetization were obtained. The transition width detected by susceptibility or magnetization (0.3 K) with an applied field of 11 Oe is slightly broader than the one detected by resistivity (0.2 K) at zero field. A previous work[17] reports a higher T_c value for $RbOs_2O_6$ single crystals, but this property is known to be strongly dependent on the sample disorder or small natural variations in stoichiometry.

The superconducting fraction of the sample was obtained from the Meissner slope of the virgin branch of $M(H)$ loops such as the one shown in Fig. 3(b). After correcting for demagnetization effects, we estimated that our samples have a superconducting fraction of 85–100 %. Together with the fact that the onset of the superconducting transition detected from susceptibility measurements coincides with the temperature at which resistance becomes negligible, this result indicates that the samples undergo a bulk superconducting transition.

In order to determine the $H-T$ vortex phase diagram of $RbOs_2O_6$ we obtained the upper critical-field line $H_{c2}(T)$ and the irreversibility line $H_{irr}(T)$ from FC-ZFC $M(T)$ measurements. Typical $M(T)$ curves for an applied field of 100 Oe are shown in Fig. 4. For all applied fields the value of the ZFC magnetization at low temperatures gives a superconducting fraction consistent with the one estimated from the Meissner slope. The temperature $T_{c2}(H)$ is determined from the onset of the superconducting behavior in the ZFC and FC branches as indicated in Fig. 4. The temperature at which the vortex magnetic response becomes irreversible on cooling $T_{irr}(H)$ is identified as the point at which both branches merge. We obtained this temperature by plotting the difference $M_{FC}-M_{ZFC}$; see Fig. 4. For each applied field, no difference in the values of T_{irr} was detected when measuring at sweep rates of 25 and 5 mK per minute. Therefore, within this measurement timescale the obtained values of T_{irr} are not influenced by any dynamical effects.

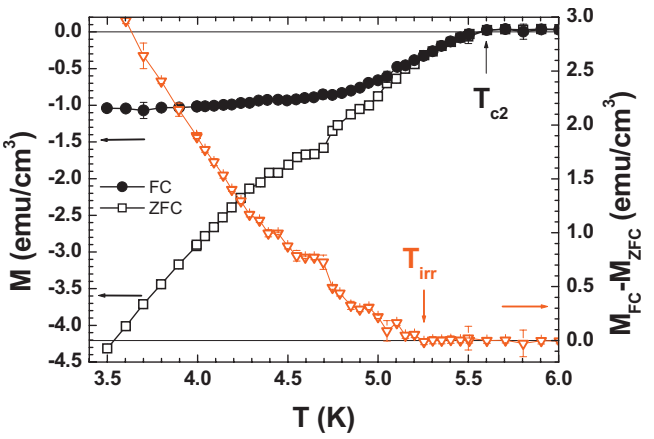

FIG. 4. (Color) Magnetization vs temperature curves of $RbOs_2O_6$ following ZFC and FC processes at an applied field of 100 Oe. The difference between both branches is considered in order to estimate the onset of the irreversible magnetic behavior at a temperature $T_{irr}(H)$. The upper critical temperature $T_{c2}(H)$ is estimated from the onset of screening.

Examples of ZFC-FC $M(T)$ curves at various applied fields are shown in Fig. 5. From the values of $T_{c2}(H)$ we obtained the upper critical field $H_{c2}(T)$ indicated in Fig. 7. In order to estimate the zero-temperature upper critical field $H_{c2}(0)$, we fit $H_{c2}(T)$ with the Werthamer-Helfand-Hohenberg model (WHH).[22–24] In the case of $RbOs_2O_6$ the Pauli paramagnetic critical field[25] $H_P\sim 18.4T_c=101$ kOe is much larger than the $H_{c2}(0)$ obtained by linearly extrapolating $H_{c2}(T)$ down to zero temperature (~60 kOe) indicating a strong spin-orbit coupling. This last condition is fulfilled when $\alpha H/H_{c2}(0)\ll\lambda_{so}$, where λ_{so} is the spin-orbit scattering

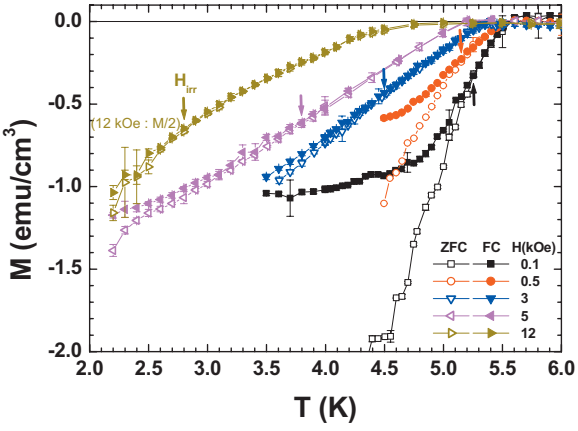

FIG. 5. (Color) Magnetization vs temperature curves of $RbOs_2O_6$ following zero-field-cooling (open symbols) and field-cooling (full symbols) processes for various applied fields. The irreversibility temperature at each field $T_{irr}(H)$ is indicated with arrows. The measurements performed at 12 kOe are shown divided by a factor of 2 for clarity.

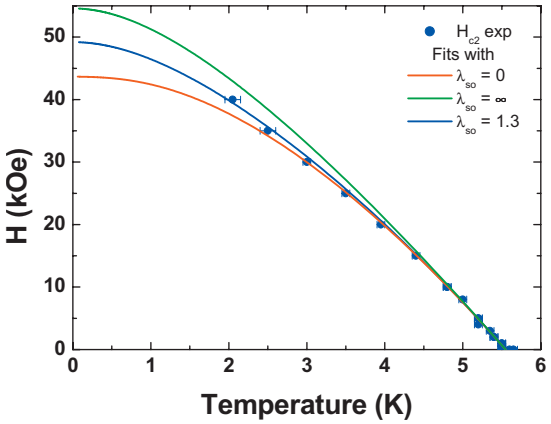

FIG. 6. (Color) Fits of $H_{c2}(T)$ with the WHH model (Refs. 22 and 23). The experimental data are shown with blue symbols. The red line corresponds to the zero spin-orbit coupling case ($\lambda_{so}=0$) whereas the green line is calculated using an infinite spin-orbit coupling ($\lambda_{so}=\infty$). The blue line is the best fit with a finite spin-orbit coupling of $\lambda_{so}=1.3\pm0.2$.

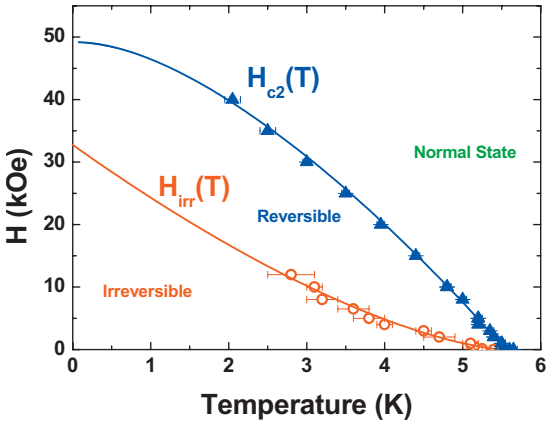

FIG. 7. (Color) Vortex phase diagram of $RbOs_2O_6$: The upper critical-field line $H_{c2}(T)$ and the irreversibility line $H_{IL}(T)$ are shown. The blue line is the best fit of the data using the WHH model (Refs. 22 and 23) which yields $H_{c2}(0)=50$ kOe. The red line is a fit of H_{irr} with a temperature dependence proportional to $(1-T/T_c)^{1.5}$.

constant and α is the Maki parameter.[26] In this limit and in the absence of magnetic impurities, the Abrikosov-Gor'kov upper critical-field equation reads (see Ref. 27 for an overview)

$$\ln\left(\frac{1}{t}\right)=\Psi\left(\frac{1}{2}+\frac{\rho_{AG}(t)}{2t}\right)-\Psi\left(\frac{1}{2}\right), \tag{1}$$

where Ψ is the digamma function, $t=T/T_c$, and $h_{c2}(t)=H_{c2}(t)/H_{c2}(0)$. The universal pair-breaking function

$$\rho_{AG}(t)=h_{c2}(t)+\frac{\alpha^2[h_{c2}(t)]^2}{\lambda_{so}} \tag{2}$$

depends on λ_{so} and α. The latter is estimated from the slope of $H_{c2}(T)$ at the vicinity of T_c: $\alpha=-0.0528\frac{dH_{c2}(T)}{dT}|_{T_c}=0.75$ (H_{c2} in kOe);[23] whereas λ_{so} is a free parameter in the fitting procedure. The best fit to the data with $\lambda_{so}=1.3\pm0.2$ is presented in Fig. 6.

The same figure shows that considering a finite spin-orbit coupling is necessary to properly fit our experimental data. The curves obtained in the extreme cases of zero ($\lambda_{so}=0$) and infinite ($\lambda_{so}=\infty$) spin-orbit coupling are shown with red and green lines. The latter curve was obtained using Eqs. (1) and (2); whereas the former was obtained considering the general Abrikosov-Gor'kov equation in the $\lambda_{so}=0$ limit.[27] It is evident that these two curves fail to properly fit the low-temperature data. The best fit to the data with $\lambda_{so}=1.3\pm0.2$ therefore indicates that in $RbOs_2O_6$ the spin-orbit coupling can be considered to be moderately strong.

The fitted $H_{c2}(0)=50$ kOe is roughly half H_P. Within the Abrikosov-Gor'kov theory we obtain a value of $H_{c2}(0)$ which is slightly smaller than that reported in Ref. 17 for other single crystals. However, in that study the zero-temperature upper critical field was estimated from a fit of $H_{c2}(T)$ with an empirical power law.[17] Our fit within the Abrikosov-Gor'kov theory yields a coherence length $\xi(0)=\sqrt{\Phi_0/2\pi H_{c2}(0)}=81$ Å. We therefore estimate a Ginzburg-Landau parameter $\kappa=31$ by considering the penetration depth value obtained from muon-spin-rotation measurements in polycrystalline samples.[28]

The vortex phase diagram of Fig. 7 also shows the locus of the irreversibility line $H_{irr}(T)$ obtained from FC-ZFC magnetization vs temperature curves. The most remarkable result shown in Fig. 7 is that the reversible magnetic response of $RbOs_2O_6$ spans an uncommonly wide region of the $H-T$ phase diagram. At low temperatures $2.5<T<4$ K, $H_{irr}(T)$ is of the order of $0.3H_{c2}(T)$. Figure 7 also shows that the irreversibility line can be well fitted with a subquadratic power law $H_{irr}\propto(1-T/T_c)^{1.5}$. These findings are in contrast with expectations for low-T_c superconductors. For example, $NbSe_2$ has a reversible region constrained to the vicinity of $H_{c2}(T)$.[29–31] Furthermore, the irreversibility line in $RbOs_2O_6$ follows the same temperature dependence as those of typical high-T_c superconductors.[32] Although there is no systematic study of the temperature evolution of the irreversibility line in KOs_2O_6 crystals in the literature, one work reports that at 5 K($t\sim0.5$) the vortex response becomes reversible at fields higher than 10 kOe ($H_{irr}\sim0.1H_{c2}$).[2] Therefore, KOs_2O_6 seems to present an even wider reversible vortex region than $RbOs_2O_6$.

An irreversible magnetic response in superconductors can have three different origins: bulk pinning, Bean-Livingston surface barriers,[33] and geometrical barriers.[34,35] In general, macroscopic magnetization measurements are not able to ascertain which of the three contributions is dominant when measuring an irreversible magnetic response that sets in at $H_{irr}(T)$. However, by conveniently modifying the sample geometry the effect of geometrical barriers can be affected. In the particular case of prismlike samples it has been shown that the effect of geometrical barriers in $H_{irr}(T)$ is negligible.[36] The Bean-Livingston surface barrier only produces a significant irreversible behavior in the case of extremely smooth surfaces.[37] In real samples with sharp corners and irregular edges, the effect of this barrier is of lesser importance. Therefore, as the crystals studied in this work

TABLE II. Measured and derived superconducting parameters for the β-pyrochlores $RbOs_2O_6$ and KOs_2O_6 and the low and high-T_c superconductors $NbSe_2$ and optimally doped $Bi_2Sr_2Ca_2Cu_3O_{10}$.

Parameter	$RbOs_2O_6$	KOs_2O_6	$NbSe_2$	$Bi_2Sr_2Ca_2Cu_3O_{10}$
$T_c[K]$	5.5[a]	9.6[b]	7.2[c,d]	110.5[e]
$\xi(0)$[Å]	81[a]	31–37[b]	77[c]	~10[e]
$\lambda(0)$[Å]	2500[f]	2500–2700[b,g]	2000[d]	500[e]
$\kappa=\frac{\lambda(0)}{\xi(0)}$	31	70–87	26	~50
γ	- [h]	~1[i]	3.3[c]	27[e]
$H_{c2}(0)$ [kOe]	50[a]	340[b]	55[c]	~3000
$G_i=0.5(\frac{k_BT_c\gamma\kappa^2}{H_{c2}(0)^2\xi(0)^3})^2$	510^{-7} [h]	510^{-6}	510^{-6}	210^{-2}
$J_c[t,h(T)]/J_0(t)$	510^{-5} [a]	510^{-6} [j]	310^{-1} [k]	110^{-5} [e]
for $h(T)=0.02$ and $t=$	0.81	0.52	0.59	0.16

[a]This work; single crystals.
[b]Ref. 11; single crystals.
[c]Ref. 39.
[d]Ref. 40.
[e]Ref. 41.
[f]Ref. 28; polycrystals.
[g]Ref. 42; polycrystals.
[h]No data available in the literature. In order to calculate G_i we assumed $\gamma=1$ (see text).
[i]Ref. 15; single crystals.
[j]Critical current calculated by us from data of Ref. 2.
[k]Ref. 30.

are prismlike, $H_{irr}(T)$ can be considered as the field at which point pinning sets in while cooling, i.e., the depinning line. Strictly speaking, the effect of pinning may become relevant at slightly lower fields than $H_{irr}(T)$.

The depinning line is determined by the competition between thermal fluctuations and pinning generated by quenched disorder naturally present in the samples.[38] The magnitude of quenched disorder is typically measured by the dimensionless critical-current density ratio $J_c(T,H)/J_0(T)$ with $J_0(T)=4c\Phi_0/12\sqrt{3}\pi\lambda^2(T)\xi(T)$ as the depairing current density.[38] For low-T_c superconductors this parameter is typically of the order of $1\times10^{-2}-1\times10^{-1}$; whereas in high-$T_c$ materials the pinning strength is weaker since $J_c/J_0\sim1\times10^{-5}-1\times10^{-2}$ at low temperatures and fields. The relevance of thermal fluctuations increases with the Ginzburg number of the material $G_i=0.5[k_BT_c\gamma\kappa^2/H_{c2}(0)^2\xi(0)^3]^2$ proportional to the electronic anisotropy $\gamma=\sqrt{m_c/m_{ab}}\geq1$.[38] Typically, $G_i\sim1\times10^{-4}-1\times10^{-8}$ for low-T_c and $\sim1\times10-1\times10^{-2}$ for high-T_c superconductors.[38] Therefore, both a small critical-current density ratio and a large Ginzburg number can conspire to produce a wide reversible vortex region.

The Ginzburg number $G_i=6\times10^{-7}$ obtained for $RbOs_2O_6$ from the $H_{c2}(0)$ estimated in this work is within the range of values typically found for low-T_c materials. To obtain this value we assumed a negligible electronic anisotropy ($\gamma=1$) based on the reported isotropic carrier mass for KOs_2O_6 (Ref. 15) and the absence of similar data for $RbOs_2O_6$. The value of G_i for $RbOs_2O_6$ indicates that thermal fluctuations are conventional and cannot account for the wide reversible vortex region. The Ginzburg number of KOs_2O_6 is one order of magnitude larger than that of $RbOs_2O_6$. This is a consequence of $H_{c2}(0)$ [$\xi(0)$] being larger (smaller) in KOs_2O_6 (see Table II for numerical details). However, this larger G_i cannot account for the greater extent of the reversible vortex region in KOs_2O_6: For example, $H_{irr}(t=0.5)/H_{c2}(t=0.5)\sim0.1$ and ~0.35 for KOs_2O_6 and $RbOs_2O_6$, respectively.

For illustrative purposes, it is very interesting to compare the case of $RbOs_2O_6$ with that of $NbSe_2$. Both compounds have similar T_c, λ, and ξ; but $NbSe_2$ is more anisotropic with $\gamma=3.3$ resulting in a Ginzburg number one order of magnitude larger than that of $RbOs_2O_6$. However, the reversible vortex region in $NbSe_2$ is constrained to 0.1 K below $H_{c2}(T)$ (Ref. 31); whereas in the case of $RbOs_2O_6$ it is much wider.

As a consequence, the wide reversible vortex region of $RbOs_2O_6$ has to be caused by a low critical-current density. We estimated the critical-current density $J_c(T,H)$ assuming that the effect of surface and geometrical barriers is negligible. In this case, within the Bean model[43] the critical-current density can be estimated from $M(H)$ loops as $J_c(T,H)\sim(c/f)\Delta M(T,H)$. Here $\Delta M(T,H)$ is the separation between the two branches of the magnetization loop at a field H, c is the speed of light, and $f=(a/2)(1-a/3b)$, where a and b are the dimensions in the plane perpendicular to the applied magnetic field. Figure 8 shows the $J_c(H)$ curves for temperatures of 4.5 and 5 K. As expected, the critical-current density decreases with magnetic field and temperature and consistently becomes negligible at the irreversibility field determined from FC-ZFC magnetization measurements.

According to the results in Fig. 8, for $RbOs_2O_6$ the critical-current density ratio $J_c/J_0\sim5\times10^{-5}$ for reduced temperature $t=4.5/T_c=0.81$ and field $h(T)=H/H_{c2}(T)=0.02$. To estimate this ratio we have calculated $J_0(t)$ considering the two-fluid model expression for $\lambda(T)$ and $\xi(T)$.[38] A similar critical-current density ratio is obtained for a reduced temperature $t=0.91$. These values of J_c/J_0 for $RbOs_2O_6$ are

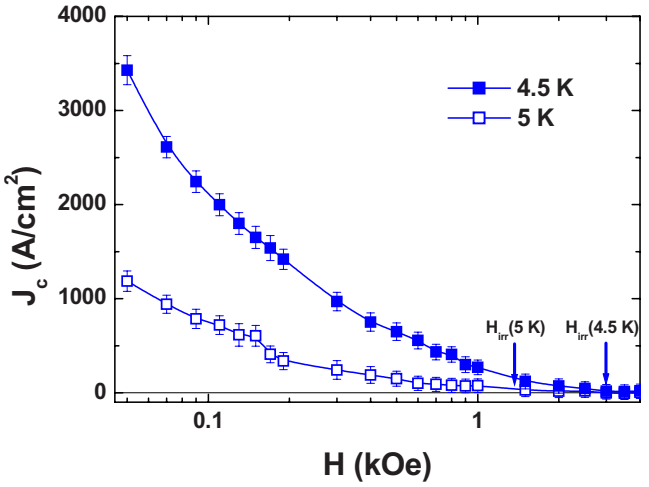

FIG. 8. (Color online) Critical-current density as a function of magnetic field for $RbOs_2O_6$ at 4.5 (full squares) and 5 K (open squares). The irreversibility fields determined from FC-ZFC $M(T)$ measurements are indicated.

smaller than values typically measured for other low-T_c materials. For example, they are four orders of magnitude smaller than that of $NbSe_2$ at the same reduced field.[30] Strikingly, the value of J_c/J_0 is comparable to that of high-T_c compounds: for example, it is of a similar order of magnitude to that of $Bi_2Sr_2Ca_2Cu_3O_{10}$ at low fields and temperatures (see Table II). Therefore, in $RbOs_2O_6$ quenched disorder has an importance as small as in the case of high T_c's. In spite of T_c being much smaller, the low value of $J_c(T,H)/J_0(T)$ is at the root of the unusually wide reversible vortex region detected in $RbOs_2O_6$.

A low magnitude of the critical-current density ratio might be generic to the β-pyrochlore family. In the case of KOs_2O_6, although no data on $J_c(T,H)$ is available in the literature, we have considered the $M(H)$ data of Ref. 2 in order to estimate its critical-current density at 5 K and $h(T)=0.02$. As shown in Table II, KOs_2O_6 has a $J_c(T,H)/J_0(T)$ one order of magnitude smaller than that of $RbOs_2O_6$. The decreased relevance of quenched disorder would explain the suspected wider reversible vortex region of KOs_2O_6.[2]

IV. CONCLUSIONS

In conclusion, we present the first data on the vortex matter phase diagram in $RbOs_2O_6$ single crystals.[17] We found that this compound presents a reversible vortex region that is unexpectedly wide for a low-T_c material. This finding might be generic to the β-pyrochlore osmate superconductors.

We found that this phenomenon originates from weak bulk pinning since the relevance of thermal fluctuations seems to be limited. The structural characterization results presented here suggest that the crystal defect density is very low in $RbOs_2O_6$. This can explain the weak pinning magnitude. Surprisingly, the Rb and K members of the β-pyrochlore family present a critical-current density ratio comparable to that of high-T_c superconductors. Furthermore, resistivity measurements in KOs_2O_6 single crystals suggest an intrinsic pinning mechanism:[7] a feature that is typically observed in high T_c's.[14] The evidence presented here therefore indicates that the negligible importance of bulk pinning produces a wide reversible region.

ACKNOWLEDGMENTS

The authors acknowledge M. Decroux, F. de la Cruz, A. A. Petrović, and G. Santi for useful discussions and A. Piriou and R. Lortz for the assistance in the SQUID measurements. This work was supported by the MaNEP National Center of Competence in Research of the Swiss National Science Foundation.

[1] E. Yonezawa, Y. Muraoka, Y. Matsushita, and Z. Hiroi, J. Phys.: Condens. Matter **16**, L9 (2004).
[2] G. Schuck, S. M. Kazakov, K. Rogacki, N. D. Zhigadlo, and J. Karpinski, Phys. Rev. B **73**, 144506 (2006).
[3] E. Yonezawa, Y. Muraoka, Y. Matsushita, and T. Hiroi, J. Phys. Soc. Jpn. **73**, 819 (2004).
[4] S. M. Kazakov, N. D. Zhigadlo, M. Brühwiler, B. Batlogg, and J. Karpinski, Supercond. Sci. Technol. **17**, 1169 (2004).
[5] M. Brühwiler, S. M. Kazakov, N. D. Zhigadlo, J. Karpinski, and B. Batlogg, Phys. Rev. B **70**, 020503(R) (2004).
[6] E. Yonezawa, Y. Muraoka, and T. Hiroi, J. Phys. Soc. Jpn. **73**, 1655 (2004).
[7] Z. Hiroi and S. Yonezawa, J. Phys. Soc. Jpn. **75**, 043701 (2006).
[8] T. Shibauchi, M. Konczykowski, C. J. van der Beek, R. Okazaki, Y. Matsuda, J. Yamaura, Y. Nagao, and Z. Hiroi, Phys. Rev. Lett. **99**, 257001 (2007).
[9] C. Dubois, G. Santi, I. Cuttat, C. Berthod, N. Jenkins, A. P. Petrović, A. A. Manuel, Ø. Fischer, S. M. Kazakov, Z. Bukowski, and J. Karpinski, Phys. Rev. Lett. **101**, 057004 (2008).
[10] Z. Hiroi, S. Yonezawa, J. I. Yamaura, T. Muramatsu, and Y. Muraoka, J. Phys. Soc. Jpn. **74**, 1682 (2005).
[11] M. Brühwiler, S. M. Kazakov, J. Karpinski, and B. Batlogg, Phys. Rev. B **73**, 094518 (2006).
[12] R. Khasanov, D. G. Eshchenko, J. Karpinski, S. M. Kazakov, N. D. Zhigadlo, R. Brütsch, D. Gavillet, D. Di Castro, A. Shengelaya, F. La Mattina, A. Maisuradze, C. Baines, and H. Keller, Phys. Rev. Lett. **93**, 157004 (2004).
[13] T. Shibauchi, L. Krusin-Elbaum, Y. Kasahara, Y. Shimono, Y. Matsuda, R. D. McDonald, C. H. Mielke, S. Yonezawa, Z. Hiroi, M. Arai, T. Kita, G. Blatter, and M. Sigrist, Phys. Rev. B **74**, 220506(R) (2006).
[14] D. Feinberg and C. Villard, Phys. Rev. Lett. **65**, 919 (1990); R. A. Doyle, A. M. Campbell, and R. E. Somekh, *ibid.* **71**, 4241 (1993).
[15] Z. Hiroi, S. Yonezawa, Y. Nagao, and J. Yamaura, Phys. Rev. B **76**, 014523 (2007).
[16] Z. Hiroi, S. Yonezawa, T. Muramatsu, J.-I. Yamaura, and Y. Mu-

raoka, J. Phys. Soc. Jpn. **74**, 1255 (2005).
[17] K. Rogacki, G. Schuck, Z. Bukowski, N. D. Zhigadlo, and J. Karpinski, Phys. Rev. B **77**, 134514 (2008).
[18] G. Sheldrick, *SHELXL-97: Program for the Refinement of DCrystal Structures* (University of Göttingen, Germany, 1997).
[19] J. Yamaura, S. Yonezawa, Y. Muraoka, and Z. Hiroi, J. Solid State Chem. **179**, 336 (2006).
[20] R. Galati, R. W. Hughes, C. S. Knee, P. F. Henry, and M. T. Weller, J. Mater. Chem. **17**, 160 (2007).
[21] Oxford Diffraction Ltd. XCALIBUR, CRYSALIS Software System, Version 1.170., 2003.
[22] E. Helfand and N. R. Werthamer, Phys. Rev. **147**, 288 (1966).
[23] N. R. Werthamer, E. Helfand, and P. C. Hohenberg, Phys. Rev. **147**, 295 (1966).
[24] A. A. Abrikosov and L. P. Gorkov, Sov. Phys. JETP **12**, 346 (1961).
[25] A. M. Clogston, Phys. Rev. Lett. **9**, 266 (1962); B. S. Chandrasekhar, Appl. Phys. Lett. **1**, 7 (1962).
[26] K. Maki, Physics (Long Island City, N.Y.) **1**, 21 (1964).
[27] Ø. Fischer, Helv. Phys. Acta **45**, 329 (1972), and references therein.
[28] R. Khasanov, D. G. Eshchenko, D. Di Castro, A. Shengelaya, F. La Mattina, A. Maisuradze, C. Baines, H. Luetkens, J. Karpinski, S. M. Kazakov, and H. Keller, Phys. Rev. B **72**, 104504 (2005).
[29] W. Henderson, E. Y. Andrei, M. J. Higgins, and S. Bhattacharya, Phys. Rev. Lett. **77**, 2077 (1996).
[30] L. A. Angurel, F. Amin, M. Polichetti, J. Aarts, and P. H. Kes, Phys. Rev. B **56**, 3425 (1997).
[31] S. Mohan, J. Sinha, S. S. Banerjee, and Y. Myasoedov, Phys. Rev. Lett. **98**, 027003 (2007).
[32] M. Tinkham, *Introduction to Superconductivity* (Dover, New York, 2004).
[33] C. P. Bean and J. D. Livingston, Phys. Rev. Lett. **12**, 14 (1964).
[34] E. Zeldov, A. I. Larkin, V. B. Geshkenbein, M. Konczykowski, D. Majer, B. Khaykovich, V. M. Vinokur, and H. Shtrikman, Phys. Rev. Lett. **73**, 1428 (1994).
[35] M. V. Indenbom and E. H. Brandt, Phys. Rev. Lett. **73**, 1731 (1994).
[36] D. Majer, E. Zeldov, and M. Konczykowski, Phys. Rev. Lett. **75**, 1166 (1995).
[37] P. G. de Gennes, *Superconductivity of Metals and Alloys* (Benjamin, New York, 1966).
[38] G. Blatter, M. V. Feigel'man, V. B. Geshkenbein, A. I. Larkin, and V. M. Vinokur, Rev. Mod. Phys. **66**, 1125 (1994).
[39] P. de Trey, S. Gygax, and J. P. Jan, J. Low Temp. Phys. **11**, 421 (1973).
[40] K. Takita and K. Masuda, J. Low Temp. Phys. **58**, 127 (1985); L. P. Le, G. M. Luke, B. J. Sternlieb, W. D. Wu, Y. J. Uemura, J. W. Brill, and H. Drulis, Physica C **185-189**, 2715 (1991).
[41] A. Piriou, Y. Fasano, E. Giannini, and Ø. Fischer, Phys. Rev. B **77**, 184508 (2008).
[42] A. Koda, W. Higemoto, K. Ohishi, S. R. Saha, R. Kadono, S. Yonezawa, Y. Muraoka, and Z. Hiroi, J. Phys. Soc. Jpn. **74**, 1678 (2005).
[43] C. P. Bean, Rev. Mod. Phys. **36**, 31 (1964).